Chemical verification of variational second-order density matrix based potential energy surfaces for the N_2 isoelectronic series

Helen van Aggelen,[1] Brecht Verstichel,[2] Patrick Bultinck,[1,a)] Dimitri Van Neck,[2] Paul W. Ayers,[3] and David L. Cooper[4]
[1]*Department of Inorganic and Physical Chemistry, Ghent University, Krijgslaan 281 S3, 9000 Ghent, Belgium*
[2]*Center for Molecular Modeling, Ghent University, Proeftuinstraat 86, 9000 Ghent, Belgium*
[3]*Department of Chemistry, Mc Master University, Hamilton, L8S 4M1 Ontario, Canada*
[4]*Department of Chemistry, University of Liverpool, L69 7ZD Liverpool, United Kingdom*

(Received 6 August 2009; accepted 28 October 2009; published online 17 March 2010)

A variational optimization of the second-order density matrix under the P-, Q-, and G-conditions was carried out for a set of diatomic 14-electron molecules, including N_2, O_2^{2+}, NO^+, CO, and CN^-. The dissociation of these molecules is studied by analyzing several chemical properties (dipole moments, population analysis, and bond indices) up to the dissociation limit (10 and 20 Å). Serious chemical flaws are observed for the heteronuclear diatomics in the dissociation limit. A careful examination of the chemical properties reveals that the origin of the dissociation problem lies in the flawed description of fractionally occupied species under the P-, Q-, and G-conditions. A novel constraint is introduced that imposes the correct dissociation and enforces size consistency. The effect of this constraint is illustrated with calculations on NO^+, CO, CN^-, N_2, and O_2^{2+}.
 [doi:10.1063/1.3354910]

I. INTRODUCTION

As the search for accurate quantum chemical methods continues, alternative descriptors to the complicated N-electron wave function have been sought. Since electrons interact pairwise the second-order density matrix (DM2) is the lowest order reduced density matrix that completely determines the energy of the system without relying on an unknown functional.[1,2] As the DM2 describes all one- and two-electron interactions, variational methods based on the DM2 seem promising, truly *ab initio* approaches. The difficulty in such optimization procedures is constraining the DM2 to correspond to a proper N-electron system during the energy minimization; this is known as the "N-representability problem."[3,4] In practice, complete N-representability is usually not feasible, and only a limited set of necessary—but not sufficient—N-representability constraints is imposed.[5,6] The resulting DM2 yields a lower bound to the exact energy. The P-, Q-, and G-conditions[3,7] have become a basic set of N-representability conditions.

An important question remains: Does the DM2 from an approximate variational calculation, using only the P-, Q-, and G-conditions for N-representability, give a correct description of a system's chemical properties? No decisive answer has been given to this question, although a few chemical properties have been studied—mainly dipole or multipole moments.[8,9] Serious shortcomings in keystone chemical properties should be addressed in order to realize the envisaged "quantum chemistry without wave functions."[10]

In a previous communication,[11] it was shown that the variational DM2 approach under the P-, Q-, and G-conditions leads to seriously incorrect dissociation limits with fractional occupation numbers on the constituent atoms. In the present paper, the 14-electron isoelectronic series, including N_2, CO, CN^-, NO^+, and O_2^{2+}, will be studied in more detail. It is well known that the subtle differences in electronegativity and ionization energy between the composing atoms present a challenge for *ab initio* methods, especially when bonds are stretched. The main purpose of this paper is to examine the performance of the DM2 method applied to the dissociation of these molecules. The chemical properties of the molecules, calculated in double-zeta basis sets, are of special interest. Potential energy surfaces calculated using the variational DM2 method will be compared to accurate *ab initio* methods, such as multireference configuration interaction (MRCI) and complete active space self-consistent field (CASSCF). For several molecules large energy differences are observed in the dissociation limit. The chemistry of the systems, examined through dipole moments as well as bond indices and atomic populations, reveals the origin of the dissociation problem. Based on these findings, a new constraint is conceived which imposes a correct dissociation.[12] This constraint is applied to the studied set of molecules, showing considerable improvement in the energy and other chemical properties at large bond lengths.

II. COMPUTATIONAL DETAILS

A semidefinite program was developed to suit electronic structure calculations, based on the logarithmic barrier method[13] to impose N-representability conditions in the outer iterations, combined with a Newton–Raphson procedure for the inner iterations. The set of imposed N-representability constraints includes the P-, Q-, and

a)Electronic mail: patrick.bultinck@ugent.be.

G-conditions, the normalization condition and conditions on spin that ensure the variationally optimized DM2 has the correct expectation value for $\hat{S}_z$ and $\hat{S}^2$. The molecules in this study are all singlets. The only data required for the variational DM2 procedure are the Hamiltonians expressed in the chosen basis, which were computed using one- and two-electron integrals from GAUSSIAN 03.[14] All calculations were carried out using the Cartesian cc-pVDZ basis set. CASSCF and MRCI reference calculations were performed with MOLPRO.[15] The active space of the full-valence CASSCF comprises ten electrons and all eight valence orbitals, and the doubly occupied inactive orbitals (mostly 1s core) were also optimized. The MRCI calculations were performed subsequently, with the full-valence CASSCF as a reference. The core (1s) orbitals were kept frozen in the MRCI expansion. Potential energy surfaces were constructed from single point calculations at a common set of internuclear distances, ranging from 0.75 to 10 Å. The calculations at 10 Å are used to represent the dissociated state. Additional DM2 calculations at 20 Å are used to check the validity of considering 10 Å to be the dissociation limit.

Expectation values, such as dipole moments and Mulliken population analysis were obtained from own routines. The quantum chemical topology (QCT) calculations needed to define the atomic domains from Bader's theory,[16] used for computing delocalization indices, were performed with PROAIM.[17]

III. THEORETICAL BACKGROUND

A. Semidefinite optimization program

In addition to the trivial requirements that the DM2 be antisymmetric, Hermitian and appropriately normalized, $\mathrm{tr}\,\Gamma = N(N-1)$, with N the number of electrons, the P-, Q-, and G-conditions are enforced. These are the best known N-representability conditions, ensuring positive semidefiniteness of the particle-particle matrix, hole-hole matrix, and particle-hole matrix, expressed in second-quantization notation as

- P condition: $\Gamma \geqslant 0$,
$$\Gamma_{ijkl} = \langle \Psi | a_k^+ a_l^+ a_j a_i | \Psi \rangle, \tag{1}$$
- Q condition: $Q(\Gamma) \geqslant 0$,
$$Q_{ijkl} = \langle \Psi | a_k a_l a_j^+ a_i^+ | \Psi \rangle, \tag{2}$$
- G condition: $G(\Gamma) \geqslant 0$,
$$G_{ijkl} = \langle \Psi | a_k^+ a_l a_j^+ a_i | \Psi \rangle, \tag{3}$$
where the indices i,j,k,l denote orthonormal spin orbitals. The first-order density matrix γ is obtained by contraction of the DM2,
$$\gamma_{ij} = \frac{1}{N-1} \sum_k^K \Gamma_{ikjk}.$$

K is the dimension of the orthonormal spin orbital basis in which the DM2 is expressed. When the anticommutation properties of creation and annihilation operators are applied to Eqs. (2) and (3), it is clear that the Q- and G-matrices are linear functions of the DM2,

$$\begin{aligned} Q(\Gamma)_{ijkl} &= \Gamma_{ijkl} + \delta_{il}\gamma_{jk} + \delta_{jk}\gamma_{il} - \delta_{ik}\gamma_{jl} - \delta_{jl}\gamma_{ik} + \delta_{ik}\delta_{jl} - \delta_{il}\delta_{jk} \\ &= \Gamma_{ijkl} + \frac{1}{N-1}\sum_n^K (\delta_{il}\Gamma_{jnkn} + \delta_{jk}\Gamma_{inln} - \delta_{ik}\Gamma_{jnln} \\ &\quad - \delta_{jl}\Gamma_{inkn}) + (\delta_{ik}\delta_{jl} - \delta_{il}\delta_{jk})\frac{1}{N(N-1)}\sum_{nm}^K \Gamma_{mnmn}, \end{aligned} \tag{4}$$

$$G(\Gamma)_{ijkl} = \delta_{jl}\gamma_{ik} - \Gamma_{ilkj} = \delta_{jl}\frac{1}{N-1}\sum_n^K \Gamma_{inkn} - \Gamma_{ilkj}. \tag{5}$$

The final expressions for $Q(\Gamma)$ and $G(\Gamma)$ are made homogeneous, allowing them to be used as a linear mapping. An orthonormal basis of matrices $\{F^I\}$ is introduced, such that the P-, Q-, and G-matrices can be written (here in vector form, index I is equivalent to a combination of orbital indices i,j,k,l),

$$\begin{aligned} \Gamma &= \sum_I \Gamma_I F^I, \\ Q(\Gamma) &= \sum_I \Gamma_I Q(F^I), \\ G(\Gamma) &= \sum_I \Gamma_I G(F^I). \end{aligned} \tag{6}$$

To ensure that the DM2 satisfies the N-representability constraints (1)–(3) in each step of the optimization process, a logarithmic barrier function is used.[13] The objective function f to be minimized is expressed as

$$f(t,\Gamma) = \mathrm{tr}[H\Gamma] - t\,\ln|\Gamma| - t\,\ln|Q(\Gamma)| - t\,\ln|G(\Gamma)|,$$

where H is the Hamiltonian matrix and t is the parameter determining the strength of the barrier. The logarithmic barrier constrains the P-, Q-, and G-eigenvalues to positive values. During the optimization, the value of t is gradually decreased toward zero. For each value of t, the optimal DM2 is calculated using a Newton–Raphson procedure. As the value of t approaches zero, the logarithmic barrier acts much like a step function, for which the optimal DM2 yields the global minimum. The gradient f′ of the objective function with respect to Γ for a fixed value of t is expressed as

$$\begin{aligned} f'_I &= H_I - t\,\mathrm{tr}[\Gamma^{-1}F^I] - t\,\mathrm{tr}[Q(\Gamma)^{-1}Q(F^I)] - t\,\mathrm{tr}[G(\Gamma)^{-1}G(F^I)] \\ &= H_I - t\,\mathrm{tr}[\Gamma^{-1}F^I] - t\,\mathrm{tr}[Q(Q(\Gamma)^{-1})F^I] \\ &\quad - t\,\mathrm{tr}[\mathcal{A}\{G(G(\Gamma)^{-1})\}F^I], \end{aligned} \tag{7}$$

where relationships (4) and (5) are used as a linear mapping. The Hermiticity of these mappings was used to derive the second line of Eq. (7). $\mathcal{A}$ stands for an antisymmetrizing operator. From the basis expansion (6) it is clear that the gradient f′ is simply $f' = H - t\Gamma^{-1} - tQ(Q(\Gamma)^{-1}) - t\mathcal{A}\{G(G(\Gamma)^{-1})\}$. A similar expression can be derived for the Hessian f″,

$$f''_{IK} = t\ \mathrm{tr}[\Gamma^{-1}F^K\Gamma^{-1}F^I] + t\ \mathrm{tr}[Q(\Gamma)^{-1}Q(F^K)Q(\Gamma)^{-1}Q(F^I)] + t\ \mathrm{tr}[G(\Gamma)^{-1}G(F^K)G(\Gamma)^{-1}G(F^I)]. \quad (8)$$

This implies that the product $f''\Delta$ used for calculating the update matrix Δ, which satisfies $f''\Delta=-f'$ can be expressed in the chosen basis of matrices $\{F^I\}$ as

$$(f''\Delta)_I = \sum_K f''_{IK}\Delta_K = t\ \mathrm{tr}\left[\Gamma^{-1}\sum_K \Delta_K F^K\Gamma^{-1}F^I\right] + t\ \mathrm{tr}\left[Q(\Gamma)^{-1}\sum_K \Delta_K Q(F^K)Q(\Gamma)^{-1}Q(F^I)\right] + t\ \mathrm{tr}\left[G(\Gamma)^{-1}\sum_K \Delta_K G(F^K)G(\Gamma)^{-1}G(F^I)\right]. \quad (9)$$

Replacing the expansion of $\Delta, Q(\Delta)$ and $G(\Delta)$ in the basis of matrices $\{F^I\}$ by the matrix itself, and applying the Hermicity of the Q- and G-mappings, leads to

$$\begin{aligned}(f''\Delta)_I &= t\ \mathrm{tr}[\Gamma^{-1}\Delta\Gamma^{-1}F^I] + t\ \mathrm{tr}[Q(Q(\Gamma)^{-1}Q(\Delta)Q(\Gamma)^{-1})F^I] + t\ \mathrm{tr}[\mathcal{A}\{G(G(\Gamma)^{-1}G(\Delta)G(\Gamma)^{-1})\}F^I],\\ f''\Delta &= t\Gamma^{-1}\Delta\Gamma^{-1} + tQ(Q(\Gamma)^{-1}Q(\Delta)Q(\Gamma)^{-1}) + t\mathcal{A}\{G(G(\Gamma)^{-1}G(\Delta)G(\Gamma)^{-1})\}.\end{aligned} \quad (10)$$

This way, the update matrix can be calculated using an iterative subspace method such as conjugate gradients or MINRES,[18] avoiding direct inversion of the Hessian, scaling as K^{12}. This method is especially advantageous when combined with a projection method to impose trace and spin conditions. The correct trace is imposed by choosing an initial DM2 with the correct trace and calculating the update matrix Δ in the space of traceless matrices. The Newton–Raphson equations $f''\Delta=-f'$ are solved using the projections $\mathcal{P}\{f''\Delta\}$ and $\mathcal{P}\{f'\}$ of $f''\Delta$ and f' onto the plane of traceless matrices,

$$\mathcal{P}\{f'\} = f' - \frac{\mathrm{tr}\, f'}{\frac{K}{2}(K-1)}\mathrm{I}.$$

The normalization condition, therefore, needs not be taken into consideration explicitly in the objective function.

Spin constraints are imposed in a similar manner. The DM2, Q- and G-matrices are expressed in a spin-coupled basis.[19] In this basis one singlet block and three triplet blocks are formed in the P-,Q-, and G-matrices. The molecules under consideration all have singlet ground states; in this case the three triplet blocks are equal. The correct spin eigenvalue is enforced by demanding that the S_z operator, expressed in the chosen basis set, forms an eigenvector of the G-matrix with eigenvalue zero,

$$GS_z = 0. \quad (11)$$

A projection operator is used to ensure the Newton equations are solved satisfying Eq. (11). This constraint imposes the inherent symmetry between the α- and β-electrons of a restricted closed-shell state, which is also known as the contraction condition. Denoting the spin of the orbital indices i,j,k,l with superscripts, the constraint for the α indices of the vector GS_z becomes

$$\begin{aligned}&(GS_z)^{\alpha\alpha}_{ij} = 0,\\ &\frac{1}{2}\sum_k^{K/2}(G^{\alpha\alpha\alpha\alpha}_{ijkk} - G^{\alpha\alpha\beta\beta}_{ijkk}) = 0,\\ &\frac{1}{N-1}\sum_k^{K/2}(\Gamma^{\alpha\alpha\alpha\alpha}_{ikjk} + \Gamma^{\alpha\beta\alpha\beta}_{ikjk}) + \sum_k^{K/2}(-\Gamma^{\alpha\alpha\alpha\alpha}_{ikkj} + \Gamma^{\alpha\beta\beta\alpha}_{ikkj}) = 0,\\ &N\sum_k^{K/2}\Gamma^{\alpha\alpha\alpha\alpha}_{ikjk} = (N-2)\sum_k^{K/2}\Gamma^{\alpha\beta\alpha\beta}_{ikjk},\end{aligned} \quad (12)$$

where N is the number of electrons.

The requirement $(GS_z)^{\beta\beta}_{ij}=0$ leads to an analogous expression for the contraction relations between the $\Gamma^{\beta\beta\beta\beta}$ and $\Gamma^{\beta\alpha\beta\alpha}$ block. As a consequence

$$\gamma^{\alpha\alpha}_{ij} = \frac{1}{N-1}\sum_k^{K/2}\Gamma^{\alpha\alpha\alpha\alpha}_{ikjk} + \frac{1}{N-1}\sum_k^{K/2}\Gamma^{\alpha\beta\alpha\beta}_{ikjk} = \frac{1}{\frac{N}{2}-1}\sum_k^{K/2}\Gamma^{\alpha\alpha\alpha\alpha}_{ikjk} = \frac{1}{\frac{N}{2}}\sum_k^{K/2}\Gamma^{\alpha\beta\alpha\beta}_{ikjk}, \quad (13)$$

which is the well known contraction condition. Condition (11) comprises the restriction on the spin eigenvalue, $\langle\hat{S}^2\rangle = S(S+1)=0$. An expression for $\langle S^2\rangle$ can be derived by applying the anticommutation rules for creation and annihilation operators to the $\hat{S}^2=\hat{S}_z^2+\hat{S}_z+\hat{S}_-\hat{S}_+$ operator,

$$\langle S^2\rangle = \frac{1}{4}(\mathrm{tr}\,\Gamma^{\alpha\alpha\alpha\alpha} + \mathrm{tr}\,\Gamma^{\beta\beta\beta\beta} - \mathrm{tr}\,\Gamma^{\alpha\beta\alpha\beta} - \mathrm{tr}\,\Gamma^{\beta\alpha\beta\alpha}) + \frac{3}{4}N - \sum_{ij}^{K}\Gamma^{\alpha\beta\alpha\beta}_{ijji}. \quad (14)$$

The notation $\mathrm{tr}\,\Gamma^{\sigma_1\sigma_2\sigma_1\sigma_2}$ is used for the trace of the $\sigma_1\sigma_2\sigma_1\sigma_2$ spin block of the DM2. By construction, $\Gamma^{\alpha\alpha\alpha\alpha}_{ijkl} = \Gamma^{\beta\beta\beta\beta}_{ijkl} = \Gamma^{\alpha\beta\alpha\beta}_{ijkl} - \Gamma^{\alpha\beta\alpha\beta}_{jikl} = \Gamma^{\beta\alpha\beta\alpha}_{ijkl} - \Gamma^{\beta\alpha\beta\alpha}_{jikl}$ for the restricted closed-shell singlet states examined here. Constraint (13) then implies that $\mathrm{tr}\,\Gamma^{\alpha\alpha\alpha\alpha}=\mathrm{tr}\,\Gamma^{\beta\beta\beta\beta}=(N/2)([N/2]-1)$, $\mathrm{tr}\,\Gamma^{\alpha\beta\alpha\beta}=\mathrm{tr}\,\Gamma^{\beta\alpha\beta\alpha}=(N/2)(N/2)$, and $\Sigma_{ij}\Gamma^{\alpha\beta\alpha\beta}_{ijji}=N/2$. Expression (14), evaluated with these traces, becomes zero. In practice, these constraints are enforced in a spin-coupled basis,[19] and the dimensions are reduced by spin symmetry. A further reduction can be made by taking the spatial symmetry into account.

B. Chemical properties and population analysis

In order to establish whether the variational DM2 method leads to a chemically correct description of the molecules, several chemical properties are computed. One of the most often considered quantities is the atomic charge. Two schemes for obtaining atomic occupancies are used here. The first is the Mulliken scheme[20] in which all electron density that originates from a basis function centered on a specific

atom is designated to this atom. Mulliken atomic charges are known to be quite basis set dependent, especially if diffuse functions are used.[21] This is not the case in the present study. Moreover, Mulliken populations are discussed primarily for large internuclear distances, where the overlap matrix is nearly block diagonal.

The results of the Mulliken population analysis are supplemented with results from Bader's QCT.[16] An important property that will be evaluated is the shared electron delocalization index (SEDI).[22] It is a measure of the extent of electron sharing between any two atoms in a molecule, providing chemists with a tool to study the phenomenon of chemical bonding in a theoretically motivated manner.[23,24] The delocalization index δ between two atoms A and B is defined as the difference between an uncorrelated distribution of the electrons and the correlated two-electron density $\rho^{(2)}$, integrated over the atomic domains Ω_A and Ω_B,

$$\begin{aligned}\delta(\mathrm{A},\mathrm{B}) &= 2\int_{\Omega_A}\rho(\mathbf{x}_1)d\mathbf{x}_1\int_{\Omega_B}\rho(\mathbf{x}_2)d\mathbf{x}_2 - 2\int_{\Omega_A}\int_{\Omega_B}\rho^{(2)} \\ &\quad\times(\mathbf{x}_1,\mathbf{x}_2)d\mathbf{x}_1d\mathbf{x}_2 \\ &= 2\mathrm{N_A}\mathrm{N_B} - 2\int_{\Omega_A}\int_{\Omega_B}\rho^{(2)}(\mathbf{x}_1,\mathbf{x}_2)d\mathbf{x}_1d\mathbf{x}_2 \\ &= 2\mathrm{N_A}\mathrm{N_B} - 2\sum_{ijkl}\Gamma_{ijkl}\mathrm{S}_{ik}^{\Omega_A}\mathrm{S}_{jl}^{\Omega_B}. \qquad (15)\end{aligned}$$

N_A and N_B are the populations obtained by integration of the density ρ over the atomic domains. The factor 2 in formula (15) stems from integration over A,B and B,A. $S_{ik}^{\Omega_A}$ denotes the overlap within the domain of atom A between orbitals i and k of the basis set in which Γ is expressed. Dipole moments for the molecules at several internuclear distances were computed from the wave functions or DM2 in the usual way.

IV. RESULTS AND DISCUSSION

The accuracy of the variational DM2 method is evaluated by comparison to accurate wave function-based methods, MRCI, and CASSCF, in the same basis set. The multiconfigurational character of CASSCF allows a good description of nondynamic correlation, which is essential to describe the dissociation process correctly. Nonetheless, MRCI data are used to complement the CASSCF data because CASSCF does not describe dynamic correlation. Is has been shown that MRCI provides an accurate approximation to full configuration interaction (FCI) for small molecules at all bond lengths.[25] The results of the DM2 calculations will be analyzed systematically, starting with potential energy surfaces, followed by a study of several chemical properties.

A. Potential energy surfaces

Figure 1 shows the energy of the studied molecules as the bond is stretched up to dissociation. Note that a logarithmic scale of basis 2 is used to give a clear picture of the bonding region as well as the dissociation limit. The difference between the DM2 energies and the MRCI energies for all molecules is given in frame (f) of Fig. 1. The results for the homonuclear diatomics N_2 and O_2^{2+} are in fair agreement with the MRCI data. Even though the DM2 energies are consistently lower, the energy graph has the correct shape. This is an important observation, especially for the O_2^{2+} ion since MP2 fails dramatically to describe its unusual potential energy surface.[26] The DM2 method correctly reproduces the energy minimum corresponding to a kinetically stable pseudobound state around 1.1 Å and the dissociation into the thermodynamically stable dissociated state $O^+ + O^+$. For the heteronuclear diatomics NO^+ and CN^-, however, serious discrepancies are observed. The DM2 energies provide a reasonable approximation near the equilibrium bond length, but as the bond dissociates the agreement with MRCI deteriorates rapidly, with energy differences up to 0.2 hartree for NO^+ at 10 Å compared to MRCI. For these molecules, the dissociation energy is much too small. Values for the dissociation energies, calculated as the energy difference between the lowest-energy molecular geometry examined here and the energy at 10 Å internuclear separation, can be found in Table III. The potential energy curve of CO does not show such increasing deviations in the dissociation limit.

These findings indicate that the dissociation process is not described properly by the DM2 minimization under P-, Q-, and G-conditions. The reason for this behavior will become clear when analyzing the atoms in the molecules.

B. Dipole moments and Mulliken population analysis

The dipole moments and Mulliken populations provide a clue to the cause of the incorrect dissociation process. Like the energy, the dipole moment is described rather well around equilibrium, but all resemblance to MRCI is lost in the dissociation limit. Table I shows MRCI and DM2 values for the component of the dipole moment along the internuclear axis at 10 and 20 Å. The center of mass was chosen as the origin. The DM2 of NO^+ shows almost no dipole moment at 10 Å although the correct dissociation into N and O^+ should produce a very large dipole moment. The dipole moment of CN^- is also substantially too small.

To gain a better understanding of this problem, a Mulliken population analysis was performed at an internuclear distance of 20 Å. In the dissociation limit, the basis function overlap matrix becomes block diagonal so the Mulliken population is the true atomic population. According to the Mulliken populations at DM2 level, NO^+ dissociates into $N^{+0.47}$ and $O^{+0.53}$ and CN^- into $C^{-0.60}$ and $N^{-0.40}$. Such dissociations are unphysical for heteronuclear molecules. Fractionally charged dissociated states can occur when the dissociation products are symmetrically equivalent, and several degenerate dissociated states with an integer charge on one of the fragments can be formed. The dissociated state with the correct symmetry will be a linear combination of those, and may result in a fractional charge on the dissociated fragments. Obviously, such symmetry is not present in heteronuclear diatomic molecules. Based on ionization energy data, the correct dissociation products for NO^+ are $N^{0.0}$ and $O^{+1.0}$; for CN^- they are $C^{-1.0}$ and $N^{0.0}$. The reference wave function-based methods give the correct dissociation products in all cases.

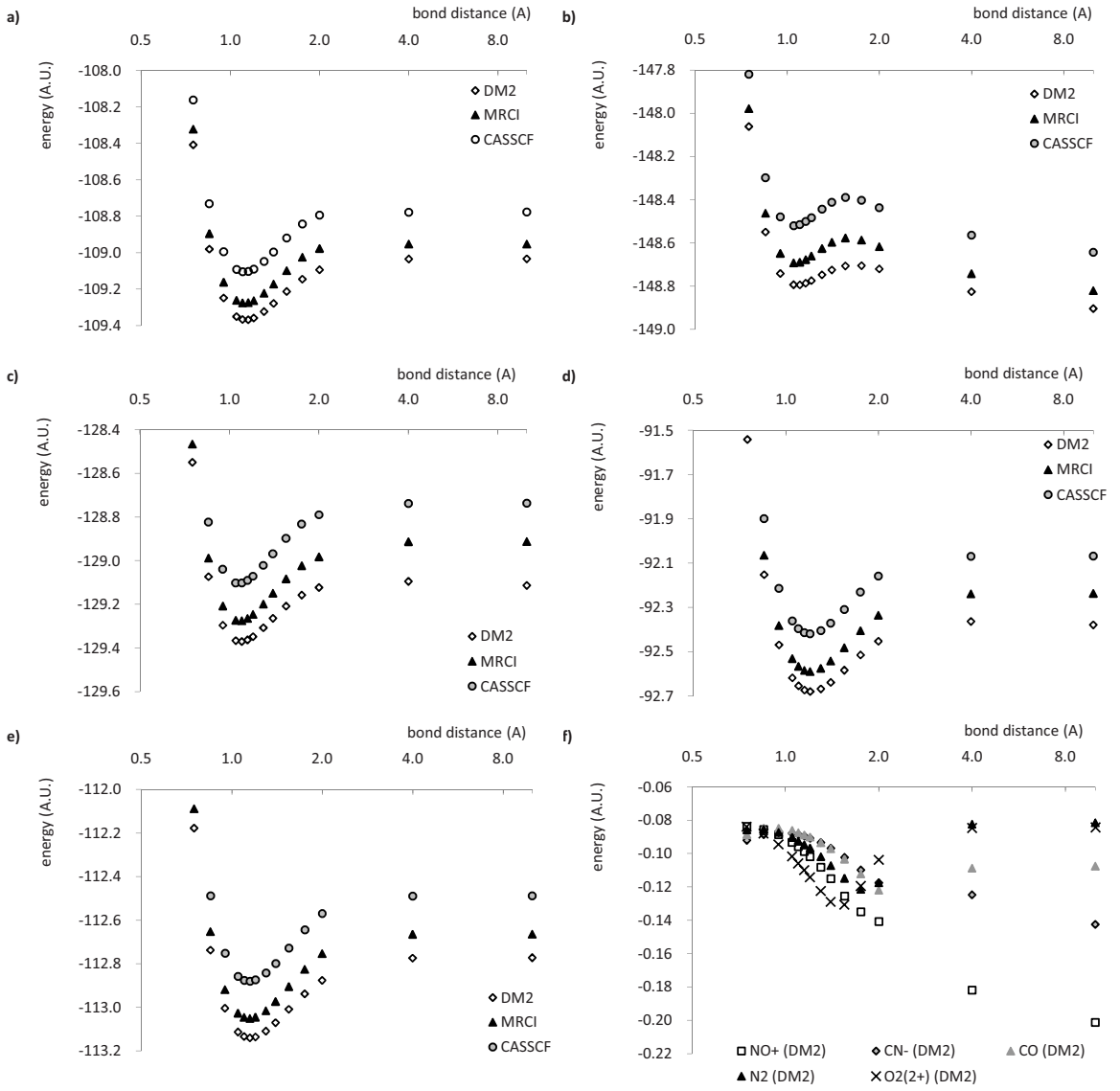

FIG. 1. Energies for (a) N_2, (b) O_2^{2+}, (c) NO^+, (d) CN^-, (e) CO as a function of the bond distance in Å, and (f) overview of the differences between the DM2 energies and the MRCI energies per molecule.

Even though the potential energy curve of CO agrees quite well with the MRCI curve, the dipole moments are wrong in the dissociation limit. Whereas the dipole moment should be nearly zero, it is still quite large at 4 Å and continues to grow as the bond length increases further. This suggests that there is still a small charge on the atoms in the dissociation limit. The Mulliken populations at 20 Å show indeed charges of 0.02 on the carbon atom and −0.02 on the oxygen atom.

C. Origin of the dissociation problem

To see what causes the dissociation problem in the heteronuclear diatomics, the energy-occupancy relationship of the composing atoms is examined in Fig. 2. Between integer electron numbers, the DM2 energy is clearly a strictly convex function of the number of electrons in each of these atoms. In density functional approximations, a similar behavior is observed, leading to fractionally occupied dissociated species.[27–29] As Perdew *et al.*[30] showed the energy-occupancy relationship should be piecewise linear since any fractionally occupied state should arise from an ensemble of integer electron states. The convex energy-occupancy relationship has an important effect on the dissociation of the molecule, which is illustrated for NO^+ in frame (d) of Fig. 2. It shows the sum of the energies of the nitrogen and oxygen atoms for a total number of 14 electrons as a function of the number of electrons on the nitrogen atom. As a consequence of the convex energy-occupancy relationship in the atoms, the minimum energy corresponds to fractionally occupied atoms. The molecule is therefore expected to dissociate into atoms with a fractional number of electrons. There is, in fact, a striking resemblance between the atomic occupations for which the sum of the atomic energies in Fig. 2(d) is minimal (determined by fitting an accurate polynomial) and the ob-

TABLE I. Dipole moments in Debije in the dissociation limit; origin chosen in the center of mass.

	MRCI (10 Å)	DM2 (10 Å)	DM2 (20 Å)
NO^+	22.39	−0.11	−0.28
CN^-	25.83	7.01	13.38
CO	0.00	−0.90	−1.71

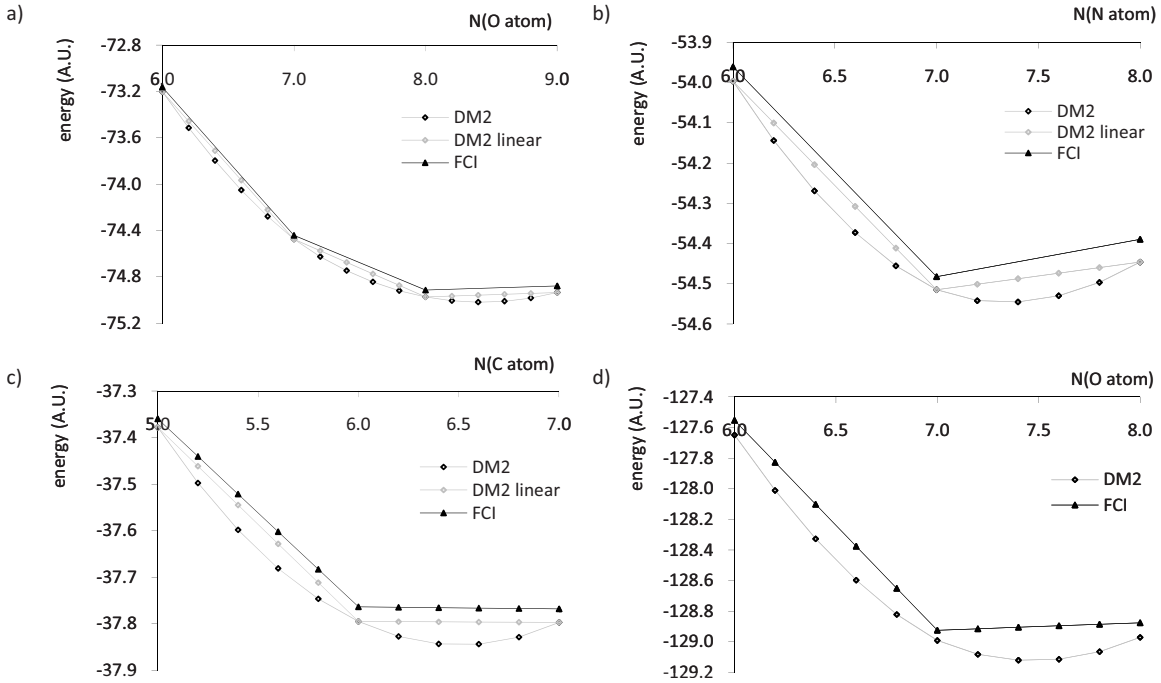

FIG. 2. Energy of the (a) N atom, (b) O atom, (c) C atom as a function of the number of electrons, and (d) summed energies of the N and O atoms corresponding to a total population of 14 electrons, as a function of the number of electrons on the N atom.

served Mulliken populations. Such resemblance is also observed for CN^- and CO. Table II shows the Mulliken populations of the molecular calculations at 20 Å and the populations corresponding to the minimum of the sum of the atomic energies.

Apart from the dissociation problem mentioned above, the issue of size consistency should be addressed. Is the molecular energy in the dissociation limit equal to the summed energies of the atoms bearing the same charges as the dissociated molecular fragments? It should be kept in mind that the electronic energy at finite bond lengths includes the repulsion between the electron clouds of the dissociated atoms, as well as the attraction energy between each nucleus and the electron cloud around the other nucleus. The molecular energies, corrected for this contribution, are compared to the sum of the atomic energies in Table II. The energy difference compared to the correct dissociation products is denoted as ΔE_1, and the difference compared to the atoms bearing the same charges as the dissociated molecular fragments is denoted as ΔE_2. Because of the dissociation into fractionally occupied atoms with too low energies, the ΔE_1 values for NO^+ and CN^- are very large. When compared to the atoms bearing the same charges as the dissociated molecular fragments, the energy difference ΔE_2 for NO^+ and CN^- is much lower. Still, the molecular energies are systematically lower than the atomic energies, implying that the P-, Q-, and G-constraints are stronger when imposed separately on the smaller atomic systems than when imposed on the 14-electron system. The variational DM2 method under P-, Q-, and G-conditions is therefore not size consistent. Following up on the results of Van Aggelen *et al.*,[11] Nakata and Yusuda[31] confirmed that the P-, Q-, and G-conditioned methods are not size extensive.

TABLE II. Mulliken populations N_1, N_2 of the dissociated molecule (20 Å); occupancies N_1', N_2' of the constituent atoms (constrained to a total of 14 electrons) for which the sum of the atomic energies is minimal, determined by fitting a polynomial; energy difference ΔE_1 between the molecular DM2 energy and the sum of the atomic DM2 energies for the correct dissociation products; energy difference ΔE_1 between the molecular DM2 energy and the sum of the atomic DM2 energies with the same populations.

	N_1, N_2	N_1', N_2'	ΔE_1	ΔE_2
N_2	7.00/7.00	7.00/7.00	−0.0035	−0.0035
O_2^{2+}	7.00/7.00	7.00/7.00	−0.0045	−0.0045
NO^+	6.53/7.47	6.51/7.49	−0.1357	−0.0041
CN^-	6.60/7.40	6.58/7.42	−0.0797	−0.0028
CO	5.98/8.02	5.98/8.02	−0.0036	−0.0034

D. Bond indices

Electron sharing indices are included in this study as they provide a valuable link between the quantum chemical description of molecules as a collection of interacting electrons and nuclei and the "classical" chemical view of molecules composed of atoms, held together by chemical bonds.[32] The calculated indices are shown in Fig. 3 for CASSCF and DM2. For MRCI, no DM2 was available to calculate SEDI values. The DM2 SEDI values capture the shape of the CASSCF SEDI graphs reasonably well. The monotonically decreasing graphs—characteristic of homonuclear diatomics in the QCT partitioning—of N_2 and O_2^{2+} are reproduced, as well as the "kinked" shape of the SEDI graphs for the heteronuclear diatomics. There are some small differences nonetheless that seem to occur systematically. The DM2 values clearly indicate a lesser degree of electron sharing in NO^+, CN^-, and CO than the CASSCF values. Moreover, the DM2 SEDI decreases somewhat faster around

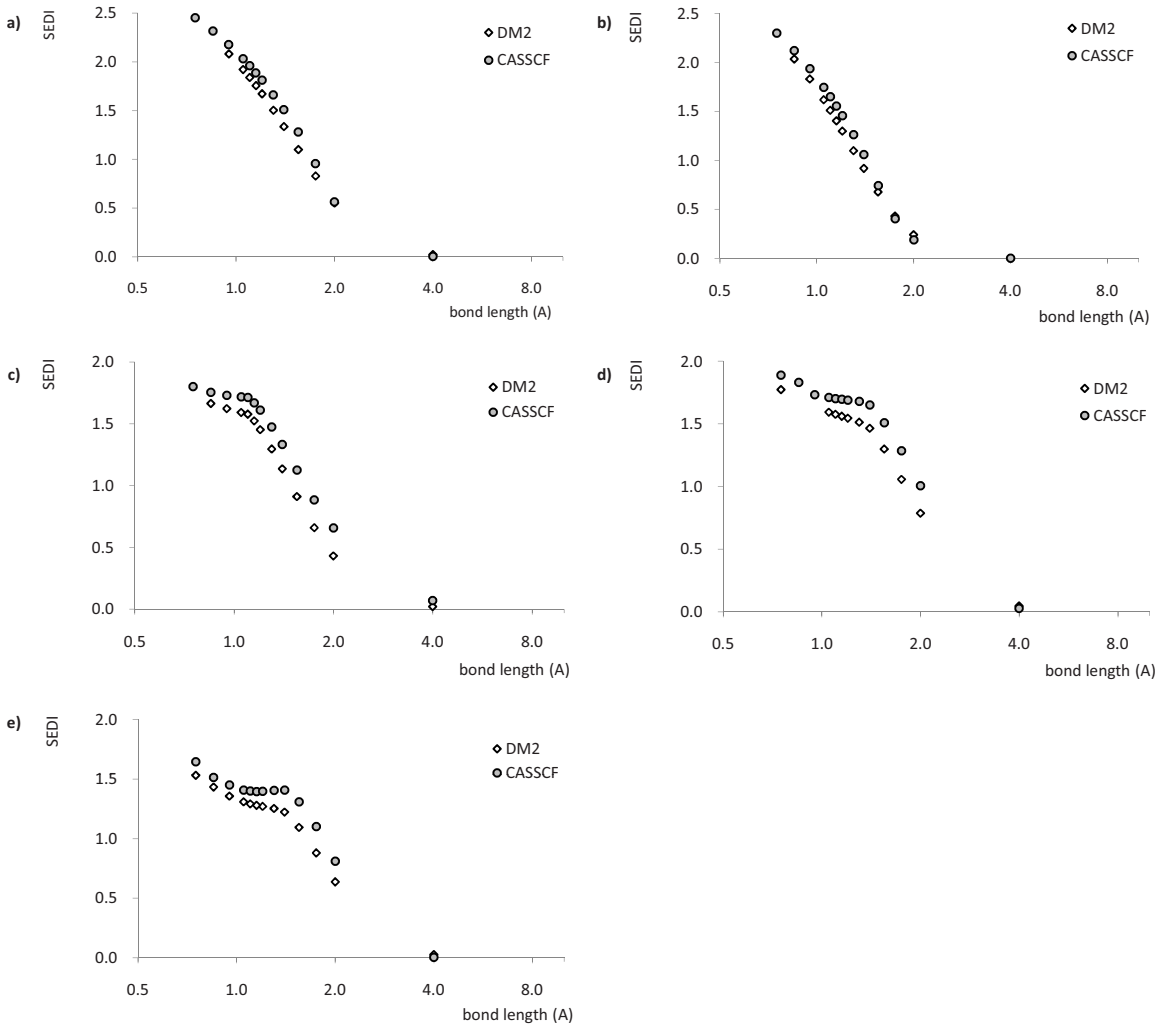

FIG. 3. SEDI for (a) N_2, (b) O_2^{2+}, (c) NO^+, (d) CN^-, and (e) CO as a function of the bond distance in Å.

equilibrium bond length; the maximum observed in the CASSCF graph for CO does not occur in the DM2 graph. In the homonuclear diatomics N_2 and O_2^{2+}, the extent of electron sharing given by the DM2 SEDI is a bit less than that indicated by the CASSCF SEDI around equilibrium bond length, but the DM2 SEDI decreases more slowly when the bond is stretched.

It is noticeable that the DM2 SEDI of all molecules decreases to zero in the dissociation limit. The dissociation problem is not reflected in the SEDI values because the DM2 electron density is localized on the atoms in the dissociation limit—although not in the right proportions.

E. Solving the dissociation problem

From the data presented in Secs. IV A–IV C it is clear that the variational method under P-, Q-, and G-conditions fails to describe the dissociation process correctly. This problem cannot be solved by adding the more stringent constraints known as T1 and T2.[33] In a previous communication[11] calculations were presented in a minimal basis, showing that the T1 and T2 constraints cause considerable improvement in the energy near equilibrium bond length, but only a minor improvement in the dissociation limit. This finding emphasizes the need of additional constraints that impose a correct dissociation.

This can be accomplished by imposing constraints on the energy of the atomic subspaces in the molecule,[12] such that the relationship between the energy and the number of electrons in the atomic subspaces cannot be strictly convex. In what follows, the subspaces are determined by the basis functions centered on each atom since the preceding analysis suggests that this choice of constraint addresses the cause of the dissociation problem. In fact, this type of constraint on the atomic subspaces is a specific instance of a more general concept since constraints can be imposed on any choice of subspace. Such subsystem constraints are justified because integer N-representability of the molecular DM2 implies fractional ensemble N-representability of any subspace DM2 and one matrix, from which constraints on the subspace energies can be derived. The theoretical background of these constraints is treated in a separate paper;[12] here we focus on the chemical consequences of the subsystem constraints.

A natural choice for the atomic subspaces is the nonorthogonal set of basis functions centered on each atom. Let K denote the dimension of the nonorthogonal spin orbital basis for the whole molecule and K_A the dimension of the nonor-

thogonal subspace for atom A. The DM2 Γ^{A} in the atomic subspace A contains all elements Γ_{ijkl} of the molecular DM2 expressed in the K-dimensional nonorthogonal basis for which i,j,k,l denote basis functions centered on atom A. Likewise, the one-matrix γ^{A} contains those elements γ_{ij} of the molecular one matrix for which the indices i,j refer to basis functions centered on A. In order to calculate subspace properties, such as the energy and population $\mathrm{N_A}$, it is desirable to express the expectation values in terms of the DM2 in the K-dimensional orthonormal molecular orbital (MO) basis $\{|\alpha\rangle\}$ used in our semidefinite program, and the operators projected onto the nonorthogonal K_{A}-dimensional subspace basis $\{|i\rangle\}$. The orthonormal MO basis is related to the nonorthogonal basis for the whole molecule through the nonunitary transformation matrix C: $|\alpha\rangle=\Sigma_i^K C_{\alpha i}|i\rangle$. For a one-electron operator $\hat{\mathrm{h}}^{\mathrm{A}}$ and a two-electron operator $\hat{\mathrm{H}}^{\mathrm{A}}$ on subspace A, the expectation values are

$$\langle \mathrm{h^A}\rangle = \sum_{ij}^{K_{\mathrm{A}}} \sum_{\alpha\beta}^{K} \gamma_{\alpha\beta} W_{\beta j} \langle j|h^{\mathrm{A}}|i\rangle W_{\alpha i}, \tag{16}$$

$$\langle \mathrm{H^A}\rangle = \sum_{ijkl}^{K_{\mathrm{A}}} \sum_{\alpha\beta\gamma\delta}^{K} \Gamma_{\alpha\beta\gamma\delta} W_{\gamma k} W_{\delta l} \langle kl|H^{A}|ij\rangle W_{\alpha i} W_{\beta j}, \tag{17}$$

where the coefficient matrix W is defined as

$$W_{\alpha i} = \sum_{k}^{K} \sum_{l}^{K_{\mathrm{A}}} C_{\alpha k} \mathrm{S}_{kl} (\mathrm{S_A^{-1}})_{li}$$

and $\mathrm{S_A^{-1}}$ is the inverse of the block $\mathrm{S_A}$ in the overlap matrix that is related to the nonortogonal basis functions in the K_{A}-dimensional subspace. From these relations a form can be obtained for the matrices $\mathrm{h^A}$ and $\mathrm{H^A}$ expressing the subspace operator in the K-dimensional orthonormal MO basis. For a more elaborate treatment of the non orthogonal subspace basis, the reader may consult the paper on the theoretical background of the subsystem constraints[12]

N-representability of the molecular DM2 implies fractional N-representability of any subspace DM2 and one matrix,[12] meaning they should be derivable from an ensemble of N-representable density matrices for integer electron numbers. This also implies that the energy for any second-order reduced Hamiltonian for the subspace must lie within the convex hull of the exact ground-state subspace energies for integer electron numbers. Considering the convex hull of exact ground-state subspace energies is contained within the convex hull of variationally optimized DM2 energies for the subspaces,

$$\begin{aligned} \mathrm{tr}[\gamma^{\mathrm{A}}\mathrm{h^A}] + \mathrm{tr}[\Gamma^{\mathrm{A}}\mathrm{V^A}] &\geq \underbrace{\min}_{x_n} \sum_n x_n E_n^{\mathrm{FCI}}(\mathrm{H^A}) \\ &\geq \underbrace{\min}_{x_n} \sum_n x_n E_n^{\mathrm{DM2}}(\mathrm{H^A}), \end{aligned} \tag{18}$$

where the electron numbers $n \in \mathbb{N}$, $\mathrm{h^A}$, and $\mathrm{V^A}$ are the one- and two-electron parts of the Hamiltonian $\mathrm{H^A}$ for atom A, $E_n^{\mathrm{FCI}}(\mathrm{H^A})$ is the exact n-electron ground-state energy for the Hamiltonian $\mathrm{H^A}$, $E_n^{\mathrm{DM2}}(\mathrm{H^A})$ is the n-electron variational DM2 energy for $\mathrm{H^A}$, and the weights $x_n \geq 0$ satisfy $\Sigma_n x_n = 1$ and $\Sigma_n x_n n = \mathrm{N_A}$. The constraints of form (18) are based on DM2 energies only so the method stays independent and internally consistent. Usually the set of energies $E_n^{\mathrm{DM2}}(\mathrm{H^A})$ for integer electron numbers n is convex, in which case the minimum energy lies on the line segment $xE_{\mathrm{N}}+(1-x)E_{\mathrm{N+1}}$ with $\mathrm{N}=\mathrm{int}(\mathrm{N_A})$. Since $x\mathrm{N}+(1-x)(\mathrm{N}+1)=\mathrm{N_A}$, Eq. (18) becomes

$$\mathrm{tr}[\gamma^{\mathrm{A}}\mathrm{h^A}] + \mathrm{tr}[\Gamma^{\mathrm{A}}\mathrm{V^A}] \geq (\mathrm{N}+1-\mathrm{N_A})E_{\mathrm{N}} + (\mathrm{N_A}-\mathrm{N})E_{\mathrm{N+1}}, \tag{19}$$

where the right-hand side gives the expected piecewise linear behavior.[30] The subsystem constraints are imposed in the form of Eq. (19). The energies E_{N} and $E_{\mathrm{N+1}}$ are calculated beforehand using the same basis set as before (the Cartesian cc-pVDZ) but without constraints on $\langle \hat{\mathrm{S}}^2\rangle$. Constraint (19) is enforced using a similar logarithmic barrier function as for the P-, Q-, and G-constraints. Fortunately, adding the subsystem constraints does not slow down calculations significantly.

The effect of the subsystem constraints is illustrated for all molecules considered. Figure 4 shows the potential energy curves when constraints of form (19) are imposed on the constituent atoms, compared to the potential energy curves of MRCI and the original P-, Q-, and G-conditioned methods. The constraint is inactive at short bond lengths and becomes active between 2 and 4 Å. The improvement in the energy at large bond lengths is considerable, up to 0.13 hartree at 20 Å for $\mathrm{NO^+}$. The dissociation energy is also greatly improved for $\mathrm{NO^+}$ and $\mathrm{CN^-}$, which can be verified from Table III. The DM2 method has a tendency to underestimate the dissociation energy, which is particularly dramatic in the case of $\mathrm{NO^+}$, where the dissociation energy is understimated by 0.1 hartree compared to MRCI. Upon addition of the subsystem constraints, this difference decreases to 0.016 hartree. Similar results are found for $\mathrm{CN^-}$; the other molecules are less affected by the subsystem constraints. Tables IV and V give the dipole moments and Mulliken populations for the heteronuclear diatomics at 4, 10, and 20 Å for the DM2 method and at 4 and 10 Å for MRCI.

The subsystem constraints force the molecule to dissociate into the correct dissociation products in the dissociation limit, which is reflected in the dipole moments and Mulliken populations. At 20 Å, $\mathrm{NO^+}$ has dissociated into a nitrogen atom and oxygen cation with near-integer occupations. Still, the dissociation into atomic species is clearly slower than for the MRCI method, for which the $\mathrm{NO^+}$ molecule already has dissociated into a nitrogen atom and oxygen cation at 4 Å.

It should be remarked that the subsystem constraints are active in $\mathrm{N_2}$ and $\mathrm{O_2^{2+}}$ too. Without the subsystem constraints, the molecular DM2 in the dissociation limit does not correspond to the antisymmetric combination of the DM2s of the separate atoms, yielding lower energies for the molecule than for the atoms at infinite separation. As the subsystem constraints enforce dissociation into correct atomic species in the dissociation limit, the variational DM2 method with the subsystem constraints is size consistent. The energy of $\mathrm{N_2}$ and $\mathrm{O_2^{2+}}$ in the dissociation limit increases upon addition of

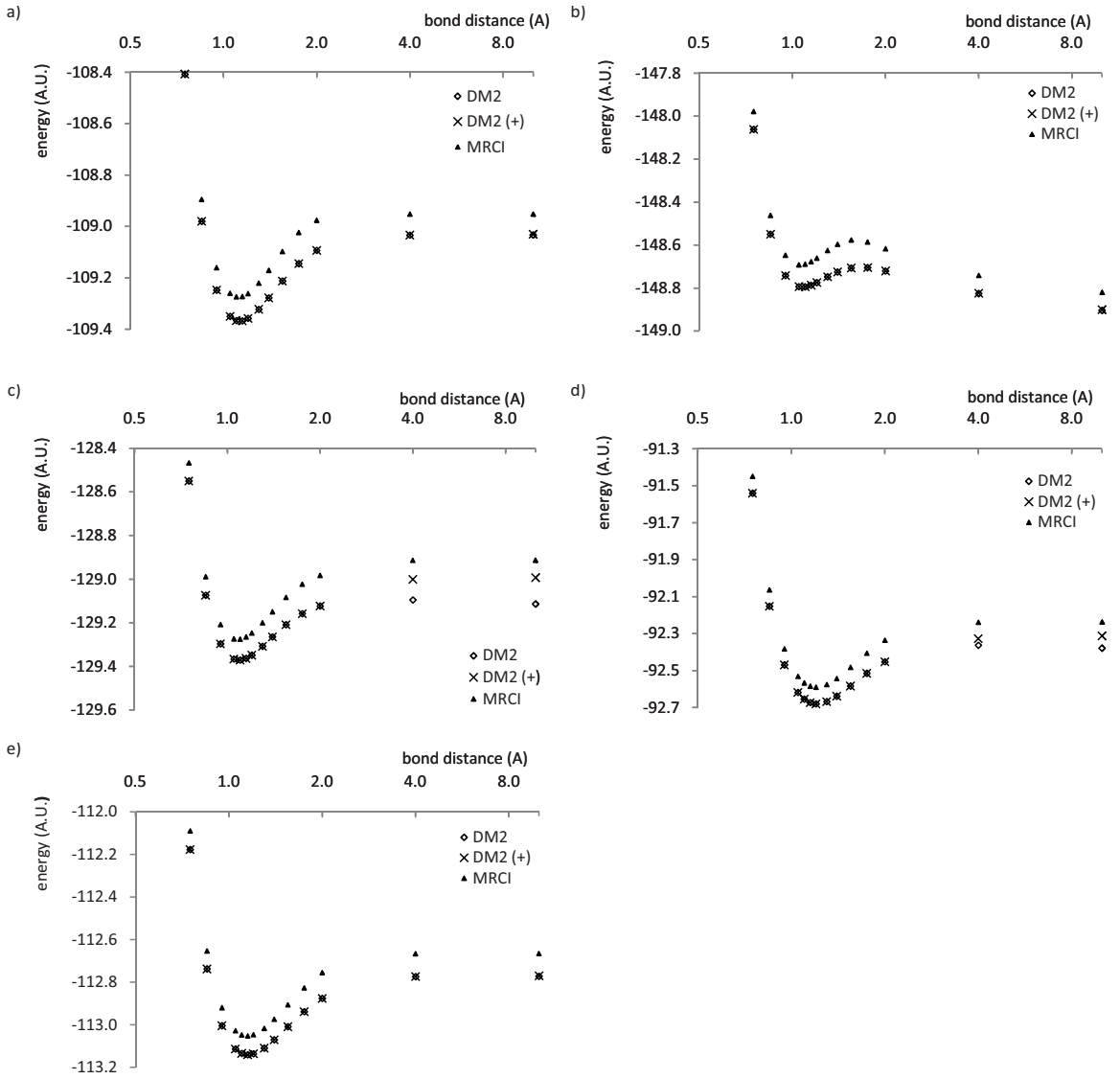

FIG. 4. Energies for (a) N_2, (b) O_2^{2+}, (c) NO^+, (d) CN^-, and (e) CO as a function of the bond distance in Å, calculated with the variational DM2 method without (DM2) and with (DM2(+)) subsystem constraints, and MRCI.

the subsystem constraints, from −148.9305 to −148.9267 hartree for O_2^{2+} at 20 Å and from −109.0332 to −109.0303 hartree for N_2 at 20 Å.

V. CONCLUSIONS

The usually applied P-, Q-, and G-conditions for N-representability are not strict enough at large bond lengths, and produce chemically unacceptable results in the dissociation limit. This problem originates from the convex relationship between the energy and the number of electrons of the atoms. Based on this finding, "subsystem constraints" were introduced. These constraints enforce a nonconvex relationship between the energy and the number of electrons of the atomic subspaces within the molecule and become active at

TABLE III. Dissociation energies (without correction for zero-point energies) for the variational DM2 method without (DM2) and with (DM2(+)) subsystem constraints and MRCI. In case of O_2^{2+}, the barrier height for dissociation is given instead.

R (Å)	N_2	O_2^{2+}	NO^+	CN^-	CO
DM2	0.335	0.089	0.257	0.301	0.368
DM2(+)	0.337	0.089	0.378	0.367	0.371
MRCI	0.322	0.116	0.362	0.353	0.387

TABLE IV. Dipole moments in Debije for NO^+, CN^-, and CO calculated with the variational DM2 method without subsystem constraints (DM2) and with subsystem constraints (DM2(+)), and MRCI.

	R (Å)	DM2	DM2(+)	MRCI
NO^+	4.0	0.07	5.68	8.76
	10.0	−0.11	20.97	22.39
	20.0	−0.29	44.18	
CN^-	4.0	3.35	7.63	9.94
	10.0	7.01	25.77	25.83
	20.0	13.38	52.11	
CO	4.0	−0.40	0.01	0.04
	10.0	−0.90	0.00	0.00
	20.0	−1.71	0.00	

TABLE V. Mulliken populations for the N atom of NO^+, C atom of CN^-, and C atom of CO calculated with the variational DM2 method without subsystem constraints (DM2) and with subsystem constraints (DM2(+)), and MRCI.

	R (Å)	DM2	DM2(+)	MRCI
NO^+	4.0	6.54	6.85	7.00
	10.0	6.53	6.97	7.00
	20.0	6.53	6.99	
CN^-	4.0	6.64	6.88	6.99
	10.0	6.61	7.00	7.00
	20.0	6.60	7.00	
CO	4.0	5.98	6.00	6.00
	10.0	5.98	6.00	6.00
	20.0	5.98	6.00	

large bond lengths. They give the correct dissociation behavior and impose size consistency for all molecules—including the homonuclear molecules. They are most effective in the cases where serious flaws occurred in the dissociation limit. For these molecules, the overall shape of the potential energy surface, dissociation energy, and dipole moment improved greatly.

ACKNOWLEDGMENTS

We gratefully acknowledge financial support from FWO-Flanders and the research council of Ghent University. P.B. acknowledges Andreas Savin and Paola Gori-Giorgi for fruitful discussions. P.W.A. acknowledges support from NSERC and Sharcnet.

[1] P. O. Löwdin, Phys. Rev. **97**, 1474 (1955).
[2] K. Husimi, Proc. Phys. Math. Soc. Jpn. **22**, 262 (1940).
[3] J. Coleman, Rev. Mod. Phys. **35**, 668 (1963).
[4] J. Coleman and V. I. Yukalov, *Reduced Density Matrices: Coulson's Challenge* (Springer-Verlag, Berlin, 2000).
[5] M. V. Mihailovlć and M. Rosina, Nucl. Phys. A **237**, 229 (1975).
[6] C. Garrod, M. V. Mihailovic, and M. Rosina, J. Math. Phys. **16**, 868 (1975).
[7] C. Garrod and J. K. Percus, J. Math. Phys. **5**, 1756 (1964).
[8] G. Gidofalvi and D. Mazziotti, J. Chem. Phys. **125**, 144102 (2006).
[9] M. Fukuda, B. J. Braams, M. Nakata, M. L. Overton, J. K. Percus, M. Yamashita, and Z. Zhao, Math. Program. Ser. B **109**, 553 (2007).
[10] C. A. Coulson, Rev. Mod. Phys. **32**, 170 (1960).
[11] H. Van Aggelen, P. Bultinck, B. Verstichel, D. Van Neck, and P. W. Ayers, Phys. Chem. Chem. Phys. **11**, 5558 (2009).
[12] B. Verstichel, H. van Aggelen, D. Van Neck, P. W. Ayers, and P. Bultinck, J. Chem. Phys. **132**, 114113 (2010).
[13] S. Boyd and L. Vandenberghe, *Convex Optimization* (Cambridge University Press, Cambridge, 2004).
[14] M. J. Frisch, G. W. Trucks, H. B. Schlegel *et al.*, GAUSSIAN 03, Revision B.05, Gaussian, Inc., Wallingford, CT, 2004.
[15] MOLPRO, a package of *ab initio* programs designed by H.-J. Werner, P. J. Knowles, R. Lindh *et al.*, version 2008.1.
[16] R. Bader, *Atoms in Molecules: A Quantum Theory* (Oxford University Press, Oxford, 1990).
[17] F. W. Biegler-König, R. F. W. Bader, and T. Tang, J. Comput. Chem. **3**, 317 (1982).
[18] C. C. Paige and M. A. Saunders, SIAM (Soc. Ind. Appl. Math.) J. Numer. Anal. **12**, 617 (1975).
[19] B. Verstichel, H. van Aggelen, D. Van Neck, P. W. Ayers, and P. Bultinck, Phys. Rev. A **80**, 032508 (2009).
[20] R. S. Mulliken, J. Chem. Phys. **23**, 1833 (1955).
[21] F. Jensen, *Introduction to Computational Chemistry* (Wiley, New York, 1999).
[22] R. Ponec and D. L. Cooper, J. Mol. Struct.: THEOCHEM **727**, 133 (2005).
[23] X. Fradera, M. A. Austen, and R. F. W. Bader, J. Phys. Chem. A **103**, 304 (1999).
[24] I. Mayer, Chem. Phys. Lett. **97**, 270 (1983).
[25] W. D. Laidig, P. Saxe, and R. J. Bartlett, J. Chem. Phys. **86**, 887 (1987).
[26] R. H. Nobes, D. Moncrieff, M. W. Wong, L. Radom, P. M. W. Gill, and J. A. Pople, Chem. Phys. Lett. **182**, 216 (1991).
[27] J. Cohen, P. Mori-Sanchez, and W. T. Yang, Science **321**, 792 (2008).
[28] P. Mori-Sánchez, A. J. Cohen, and W. T. Yang, J. Chem. Phys. **125**, 201102 (2006).
[29] J. P. Perdew, A. Ruzsinszky, G. I. Csonka, O. A. Vydrov, G. E. Scuseria, V. N. Staroverov, and J. M. Tao, Phys. Rev. A **76**, 040501 (2007).
[30] J. P. Perdew, R. G. Parr, M. Levy, and J. J. L. Balduz, Phys. Rev. Lett. **49**, 1691 (1982).
[31] M. Nakata and K. Yusuda, Phys. Rev. A **80**, 042109 (2009).
[32] I. Mayer, J. Math. Phys. **28**, 204 (2007).
[33] R. M. Erdahl, Int. J. Quantum Chem. **13**, 697 (1978).